Appl. Phys. B (2015) 119:371–380
DOI 10.1007/s00340-015-6085-1

Applied Physics B
Lasers and Optics

Effects of turbulent flow field on wavefront aberration in liquid-convection-cooled disk laser oscillator

Peilin Li[1] · Xing Fu[1] · Qiang Liu[1] · Mali Gong[1]

Received: 27 November 2014 / Accepted: 11 March 2015 / Published online: 22 March 2015

Abstract A liquid-convection-cooled Nd:YAG disk laser oscillator with an output power of 30.7 W and a slope efficiency of 14.1 % is built. By using large-eddy simulation model, the wavefront aberration induced by the turbulent flow is numerically calculated. In the experiment, a Shack–Hartmann wavefront sensor is used to measure the wavefront aberration and the laser intensity distribution. The RMS values and PV values of the beam wavefront and the phase stability of three feature points have been investigated. The experimental results prove that the turbulent flow with high flow velocity and high turbulent intensity can reduce the aberration of the flow field.

1 Introduction

Various application demands of diode-pumped solid-state laser (DPL) make the scientific researchers of this field devote continuously to the improvement of output power and beam quality [1–3]. High-power DPL has recently attracted much interest due to its compact structure, high efficiency, power scalability, and good operation stability. However, solid-state gain medium generates heat when being pumped by high-power diode laser. Thermal effects, such as thermally induced stress birefringence and thermal lens, limit the output power and beam quality of solid-state lasers, while extremely high thermally induced stress can even cause the fracture of the gain material [4–7].

✉ Qiang Liu
lipl11@mails.tsinghua.edu.cn

[1] Department of Precision Instrument, Center for Photonics and Electronics, State Key Laboratory of Tribology, Tsinghua University, Beijing 100084, China

Recently, it has been suggested that there may be an optimal solution for high-power DPL while combining the thin-disk configuration and the cooling method that the laser gain medium is directly convection-cooled by the liquid. The thin-disk laser has been proven to be an effective configuration to reduce thermal effects, because of its large cooling surface and short spacing between the cooling surface and the heat source [8, 9]. In 2008, General Atomics Corp proposed the "liquid laser" scheme that has the coolant liquid directly flowing over the surfaces of thin-disk laser material, expecting to realize 150 kW continuous-wave (CW) output power [10]. In 2010, by employing Nd:YAG ceramic thin slab as laser material and using the scheme that coolant liquid directly flows over the slab surfaces, Textron Defense Inc presented 27 kW CW output produced by a single-laser module and 100 kW CW output produced by six laser modules [11]. From the schemes of General Atomics Corp and Textron Defense Inc, it can be seen that the cooling surface coincides with the laser transmission surface, leading to a challenge that the liquid flow exerts influence on the wavefront aberration of the laser beam that passes through the flowing coolant liquid, which may degrade the beam quality [12].

Solid-state laser gain medium generates heat when being pumped by high-power diode laser. Though the gain medium is directly convection-cooled, the heat is transferred into the water and generates temperature gradient in flow field. Turbulent flow brings about a perturbation on the temperature field. The refractive index field varies primarily with the temperature field. Since the refractive index field is inhomogeneous, the laser beam passing through the liquid flow field is distorted. However, there have rarely been experiment reports about the laser wavefront aberration induced from the coolant flow field.

In this paper, the wavefront aberration induced by the turbulent flow field in liquid-convection-cooled disk laser is studied in detail, by ways of both simulation and experiment. Firstly, the wavefront aberration induced by the flow field is numerically calculated. By using large-eddy simulation model and integrating the thermal-induced variations of the refractive index along the laser beam path, the two-dimensional wavefront aberration is simulated, indicating that enhancing the flow velocity on laser material surfaces can reduce the aberration. Then, an experimental setup of liquid-convection-cooled disk laser oscillator is built, while a Shack–Hartmann wavefront sensor is used to measure the wavefront aberration and the laser intensity distribution. Wavefront aberration of output laser at different coolant flow velocity is experimentally studied, which also proves that the turbulent flow with high-speed flow velocity and high turbulent intensity can reduce the aberration. This study on wavefront aberration induced by the flow field is of great importance for developing high-power liquid-convection-cooled disk lasers. However, some aspects of this study can be applied in many research fields such as dye lasers, beam propagation through turbulent atmosphere, underwater laser communication.

2 Experimental setup

The experimental setup of the liquid-convection-cooled disk laser oscillator is depicted in Fig. 1. The laser gain medium is a 1.0 at.% doped Nd:YAG disk. The dimension of the disk is 50 × 30 × 5 mm^3 (length × width × thickness), with a large aperture (50 × 30 mm^2) for light passage. The end surface that the pump light first enters is AR coated at both 808 and 1064 nm (relative to water), and the other end surface is AR coated at 1064 nm (relative to water) and high-reflection (HR) coated at 808 nm (relative to water). Thus, the pump light passes the crystal for two times, with the absorption efficiency estimated as 95.0 %. The Nd:YAG thin disk is supported in a water-filled chamber with two quartz windows. Each quartz window has one side AR coated relatively to air for both 808 and 1064 nm, and the other side AR coated relatively to water for 808 and 1064 nm.

The de-ionized water, of which the temperature and the flow velocity are adjustable, is used as the cooling liquid. The cooling liquid passes through the chamber from the inlet to the outlet, flowing all over the surfaces of the gain medium, especially the two large 50 × 30 mm^2 apertures. With the coolant water flowing over the laser transmission surface directly, there is a force convection heat transfer between the coolant water and the disk. The distances between the disk large

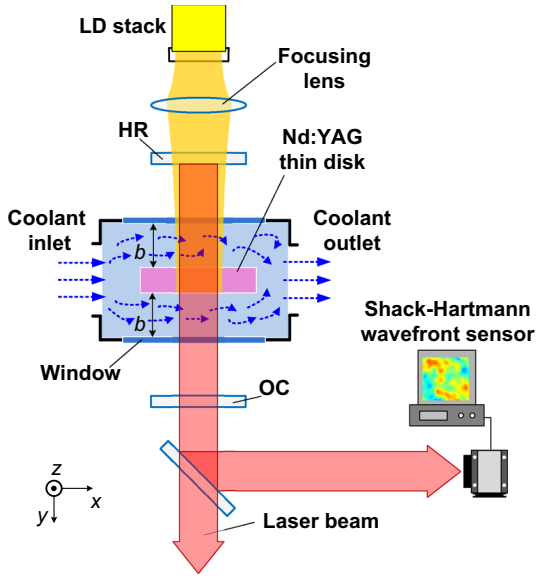

Fig. 1 Experimental setup of the liquid-convection-cooled disk laser oscillator

surfaces and the windows are $b = 2$ mm, and the water is flowing along the positive direction of the x axis. The convective heat transfer coefficient of a turbulent flow is higher than that of a laminar flow. In order to conduct out the heat generated within the disk more rapidly and prevent the fracture of the gain material, the flow is kept in the state of turbulence.

The disk is end-pumped from single side by a laser diode array (LDA), which is capable of producing an output power of up to 1000 W (at the current of 100 A) at 808 nm. The LDA, consisting of 10 laser diode bars, is collimated in fast axis by microlens but not in slow axis, corresponding to the fast-axis divergence angle of 2° and the slow-axis divergence angle of 8°. The pump light after focusing enters the gain medium, with a square-shaped pump spot of 7 × 7 mm^2 on the disk end surface. A flat–flat cavity is used in the laser resonator, with a cavity length of 70 mm. The resonator consists of a total-reflection plane mirror (HR) and an output coupler (OC). The plane output coupler of 95 % transmission is positioned at a distance of 40 mm from the disk surface. In the resonator, the large-aperture laser beam at a wavelength of $\lambda = 1064$ nm goes through the Nd:YAG disk, two quartz windows and two water layers. The wavefront of laser beam is measured by a Shack–Hartmann wavefront sensor, with an aperture size of 6.1 × 4.9 mm^2, a pixel size of 4.65 × 4.65 μm^2 and a lenslet array count of 40 × 32. The damage threshold of the Shack–Hartmann wavefront sensor is 0.1 mW/cm^2. Therefore, a partially reflecting mirror and an optical attenuator are used to weaken the power density of the output beam.

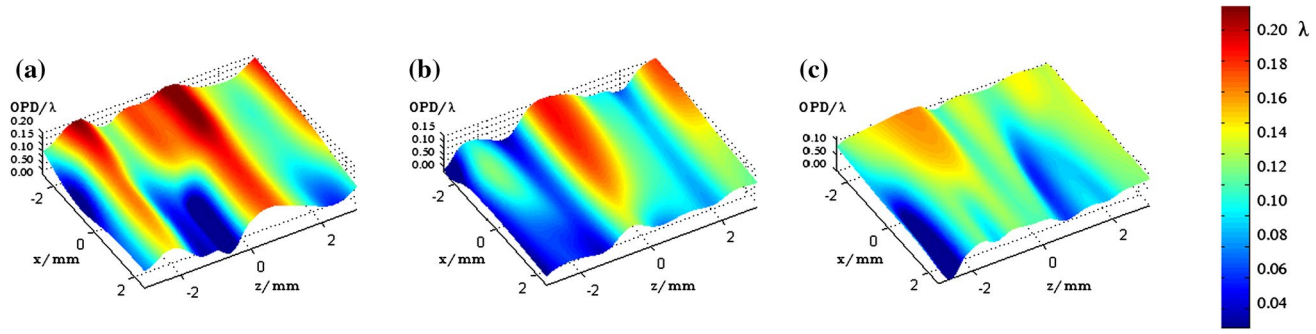

Fig. 2 Simulated two-dimensional wavefront aberrations when flow velocity is **a** 1 m/s, **b** 2 m/s, and **c** 5 m/s

3 Experiment results and discussion

3.1 Numerical simulation

The cooling water under discussion is a typical example of Newtonian fluids, and its flow field can be obtained by solving Navier–Stokes (NS) equations of Newtonian fluids. Assuming the fluid properties are constant and the flow is three-dimensional, the hydrodynamic equations governing the turbulent flow field and the heat transfer process are given in terms of continuity equation (Eq. 1), momentum equations (Eq. 2) and energy equations (Eq. 3).

$$\frac{\partial \rho}{\partial t} + \mathrm{div}(\rho \mathbf{u}) = 0, \tag{1}$$

$$\frac{\partial (\rho u_i)}{\partial t} + \mathrm{div}(\rho u_i \mathbf{u}) = -\frac{\partial p}{\partial x_i} + \mathrm{div}(\mu \mathrm{grad} u_i), \tag{2}$$

$$\frac{\partial (\rho T)}{\partial t} + \mathrm{div}(\rho T \mathbf{u}) = \mathrm{div}\left(\frac{k}{c_p}\mathrm{grad} T\right), \tag{3}$$

where in this case $\mathbf{u}$ is the flow velocity vector, u_i is the velocity component in x, y or z direction, p is the pressure, and T is the temperature distribution. Assuming the water temperature of 20 °C, we have the dynamic viscosity coefficient of $\mu = 0.001003$ kg/ms, the heat conductivity of $k = 0.6$ W/m K, and heat capacity of $c_p = 4182$ J/kg K [13].

To numerically solve the NS equations in three-dimensional turbulent flow field, large-eddy simulation (LES) model is adopted in this paper. In LES model, the instantaneous NS equations are low-pass-filtered by subgrid-scale (SGS) model [14, 15].

When being pumped by the high-power LDA, disk-type gain medium generates vast amounts of heat, which is expressed as a fraction of the absorbed pump power deposited as heat (30 % for Nd:YAG). With the pump power of 265 W, the average pump power density on surfaces of the disk is 541 W/cm^2. In the modeling, the inlet coolant temperature is 20 °C, and the outlet coolant pressure is 0.1 MPa. The entrance velocity values are assumed as $u_0 = 1$, 2 and 5 m/s, and the Reynolds number is calculated as

$$Re = \frac{u_0 D_\mathrm{h}}{v}, \tag{4}$$

where $D_\mathrm{h} = 2b$ is the hydraulic diameter of the channel between two parallel plates and v is the kinematic fluid viscosity coefficient of water, defined as $v = \mu/\rho$. According to Eq. 4, the Reynolds numbers are calculated to be 3980, 7960 and 19,900, respectively. The Reynolds numbers are much higher than the critical Reynolds number as 2300; therefore, the flow is in the state of turbulence. In addition, Reynolds numbers are the representation of turbulence intensity, while high Reynolds number corresponds to high turbulent intensity and strong turbulence perturbation on the flow field.

According to the calculation results of LES model, the instantaneous velocity field and temperature field are calculated. The wavefront aberration is quantitatively evaluated by optical path difference (OPD). The OPD induced by the flow field is obtained by integrating the thermal-induced variations of the refractive index along the laser beam path within the flowing water.

$$\mathrm{OPD} = \frac{\mathrm{d}n}{\mathrm{d}T}\int_l (T - T_0)\mathrm{d}l, \tag{5}$$

where T_0 is the inlet coolant temperature, l is the length of beam path, $\mathrm{d}n/\mathrm{d}T = -1.3 \times 10^{-4}$ K^{-1} is the temperature coefficient of the refractive index for water.

The wavefront aberration of the laser beam with an aperture of 5 mm × 5 mm is calculated after passing through two 2-mm-thick fluid layers. Figure 2 demonstrates two-dimensional wavefront aberrations with the flow velocity of $u_0 = 1$, 2 and 5 m/s at time $t = 1$ s.

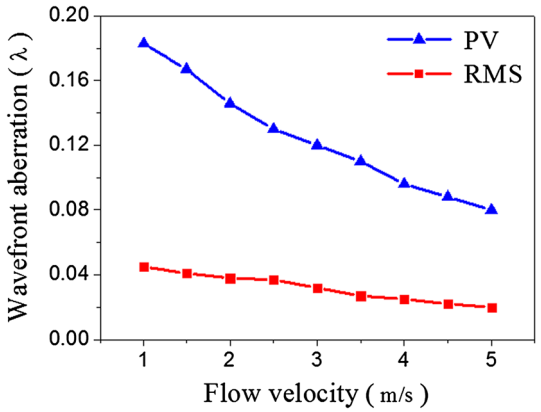

Fig. 3 PV value and RMS value of wavefront aberration versus turbulent flow velocity

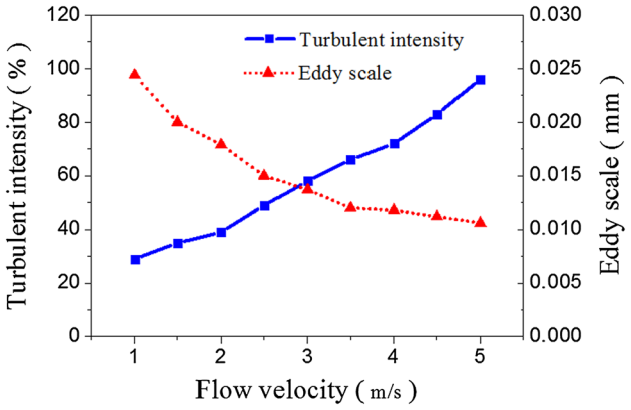

Fig. 4 Turbulent intensity and eddy scales of the flow field versus turbulent flow velocity

The peak-to-valley (PV) values and root mean square (RMS) values of wavefront aberrations are demonstrated in Fig. 3 versus the flow velocity of coolant liquid. For each of given PV values and RMS values, ten statistically independent simulations are conducted. Each of the scattering points in Fig. 3 represents the average value of ten times of simulation. The simulation results demonstrate that with the increase in flow velocity, the PV value and the RMS value decrease, indicating that enhanced flow velocity on the laser material surfaces serves to reduce the wavefront aberration.

When the flow is turbulent, the instantaneous flow velocity component u_i can be divided into two parts, as given by

$$u_i = \bar{u}_i + u_i' \tag{6}$$

where $\bar{u}_i$ is the mean value of flow velocity and u_i' is the actual velocity fluctuating component. The turbulence intensity, also often referred to as turbulence level, is defined as:

$$I = \frac{\left[\overline{(u_i')^2}\right]^{1/2}}{|\overline{u_i}|} \tag{7}$$

where the numerator is the RMS of the turbulent velocity fluctuations and the denominator is the absolute value of the mean velocity. Turbulent kinetic energy is the mean kinetic energy per unit mass associated with eddies in turbulent flow. Physically, the turbulence kinetic energy is characterized by measured RMS velocity fluctuations, which is written as

$$\kappa = \frac{1}{2}\overline{(u_i')^2}. \tag{8}$$

Turbulence dissipation rate is the rate at which turbulence kinetic energy is converted into thermal internal energy, which is used as given by

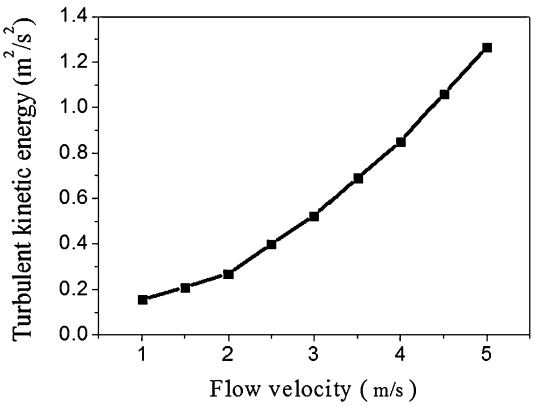

Fig. 5 Turbulent kinetic energy of the flow field versus turbulent flow velocity

$$\varepsilon = \frac{\mu}{\rho}\overline{\left(\frac{\partial u_i'}{\partial x_k}\right)^2} \tag{9}$$

where in this case μ is the dynamic viscosity coefficient and ρ is the density of liquid. The Kolmogorov turbulence theory introduces a Kolmogorov length scale to describe the scales in the spectrum that form the viscous sub-layer range. At the Kolmogorov scale, viscosity dominates and the turbulent kinetic energy is dissipated into heat. They are defined by

$$\eta = \left[\frac{(\mu/\rho)^3}{\varepsilon}\right]^{1/4} \tag{10}$$

where ε is the turbulence dissipation rate, μ is the dynamic viscosity coefficient, and ρ is the density. In this paper, the Kolmogorov length scale η is used to evaluate the eddy scale of turbulence flow [16].

According to the calculation results of simulation model, the turbulent intensity, eddy scales and turbulent kinetic energy of the flow field are calculated. The turbulent intensity and eddy scales of the flow field versus turbulent flow velocity are illustrated in Fig. 4. The turbulent intensity is 29 % when the flow velocity is 1 m/s. The turbulent intensity gets stronger as the turbulent flow velocity increases, and reaches 96 % at the flow velocity of 5 m/s with the absolute value enhanced more than two times. This discloses that the turbulence level turns form weak to violent with the flow velocity increases. In addition, the calculation of eddy scales indicates that with the increase in turbulent intensity, the eddies with large-scale break up and the eddy scales decrease. The turbulent kinetic energy versus the flow velocity of coolant liquid is demonstrated in Fig. 5, indicating that with the increase in flow velocity the turbulent kinetic energy enhances. Each of the scattering points in Figs. 4 and 5 represents the average value of ten times of statistically independent simulation.

The beam scattering effect induced by turbulent eddies can be explained by the random lens model [17]. The turbulent eddies are considered as random negative lens, which are randomly distributed in the flow field. By examining the behavior of a single lens, then accounting for the large number of random lenses, we can develop a physical understanding of the beam scattering effect induced by turbulent eddies. Assume that the eddy scale is η and the refractive index difference is Δn, the focal length of the random lens is estimated as

$$f = \frac{\eta}{\Delta n}. \tag{11}$$

When the flow velocity are 1 and 5 m/s, the eddy scale η is 0.0244 and 0.0106 mm, while the temperature difference of the flow field are 65 and 20 °C, which result in that the refractive index difference Δn of the flow field is 8.45×10^{-3} and 2.60×10^{-3}. Therefore, when the flow velocity increases from 1 to 5 m/s, the focal length enhances as well from 2.89 to 4.08 mm. Longer focal length of the negative lens corresponds to weaker scattering effect of turbulent eddies. Therefore, the beam scattering effect decreases because the temperature gradient at thermal boundary layer weakens and the temperature difference decreases at high turbulent flow rate.

3.2 Experiment result and discussion

We suppose that there are two effects of flow velocity on wavefront aberration. The first is that high flow velocity brings about a great perturbation on the temperature field, which tends to increase the wavefront aberration. The second is that high flow velocity enhances the heat transfer on disk surfaces, leading to a small temperature gradient at thermal boundary layer, which tends to reduce the wavefront aberration. Therefore, the two effects exert opposite influence in terms of changing the wavefront aberration. The simulation results indicate that the second effect plays a major role and the fast turbulent flow velocity with high turbulent intensity can reduce the aberration. However, it is essential for the result to be proved in the experiments.

Laser outputs are successfully obtained in the experiment of the liquid-convection-cooled disk laser oscillator. With a pump spot of 7×7 mm^2 at the disk center, an inlet coolant temperature of 20 °C and a cooling flow velocity of 5 m/s, 30.7 W of CW output power is achieved at the maximum pump power of 265 W, corresponding to the optical–optical efficiency of 11.6 % and the slope efficiency of 14.1 %.

The optical–optical efficiency is quite low, because there are two layers of the coolant liquid in the laser cavity, which introduce an extra absorption loss and a scattering loss of the laser and reduce the optical–optical efficiency. The single-pass loss σ of the cavity can be calculated as

$$\sigma = 1 - \exp\left[-(\alpha + s)l\right] \tag{12}$$

where α is the absorption coefficient of de-ionized water at 1064 nm which is measured as 1.43×10^{-1} cm^{-1} [9], $s = 1.05 \times 10^{-6}$ cm^{-1} is the scattering coefficient of de-ionized water at 1064 nm [18], and $l = 4$ mm is the total thickness of the coolant liquid layers. It is clear that the absorption coefficient is 5 orders greater in magnitude than the scattering coefficient. Therefore, the single-pass cavity loss is mainly caused by the absorption loss, which is calculated as 5.56 % using Eq. 12.

Through the experiment, it is found that the single-pass cavity loss has almost no correlation with the turbulent intensity when the coolant flow velocity varies in the range of 1–5 m/s. This confirms that the scattering loss induced by the turbulence is negligible in comparison with the absorption loss. The single-pass cavity loss is measured as 5.53 % in this experiment, which is in good agreement with the calculation result 5.56 %.

The efficiency will be further improved if a specific liquid with little absorption at 1064 nm is used as the cooling liquid instead of the de-ionized water. The absorption coefficients at 1064 nm of the heavy water (D_2O) with different deuteration degree are measured using a spectrometer, while the results are depicted in Fig. 6, together with the calculated single-pass cavity loss. The heavy water with the deuteration degree of 99.8 % that has an extremely small absorption coefficient of 2.3×10^{-2} cm^{-1} at 1064 nm is an ideal cooling liquid. According to the calculation, the single-pass cavity loss will reduce to 0.916 % if the heavy water with the deuteration degree of 99.8 % is used as the cooling liquid.

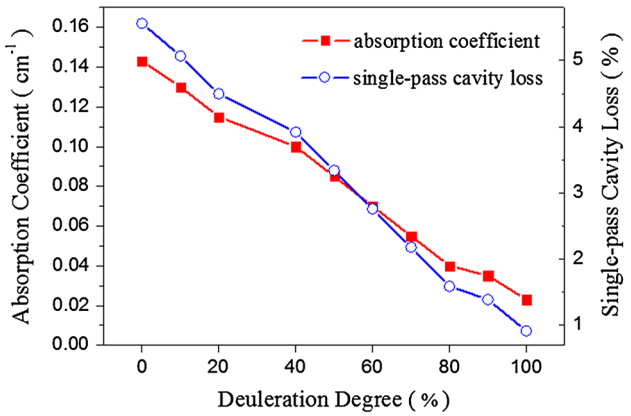

Fig. 6 Absorption coefficient at 1064 nm and the single-pass cavity loss versus the deuteration degree of the heavy water

The spot size of the near-field laser pattern is around 5×5 mm^2. The near-field patterns of the output laser when flow velocity $u_0 = 1$, 2 and 5 m/s are shown in Fig. 7. The laser pattern deteriorates on the direction orthogonal to the coolant flow direction. With the increase in turbulent flow velocity, the beam profile is improved to an approximate circle shape.

Figure 8 demonstrates the wavefront aberration of output laser in the experiment measured by the Shack–Hartmann wavefront sensor, in different coolant flow velocity condition that $u_0 = 1$, 2 and 5 m/s.

It should be noted that wavefront distortion due to first-order to sixth-order polynomials is not included and displayed in the analysis of wavefront distortion. The wavefront distortion due to turbulent flow is described by high-order Zernike polynomials. The piston and tilt components (first-order to third-order polynomials) can be easily eliminated. The defocus component (fourth-order polynomials) is nothing but a curvature on the wavefront analogous to an ideal lens. The astigmatism components (fifth-order to sixth-order polynomials) are mainly caused by different divergence angles of the pump laser in fast axis and low axis. As a consequence, the acquisition and diagnostics of high-order distortions is of great importance. It is demonstrated in Figs. 7 and 8 that the influence of flow velocity on wavefront aberration is very obvious. The experiment results indicate that the fast turbulent

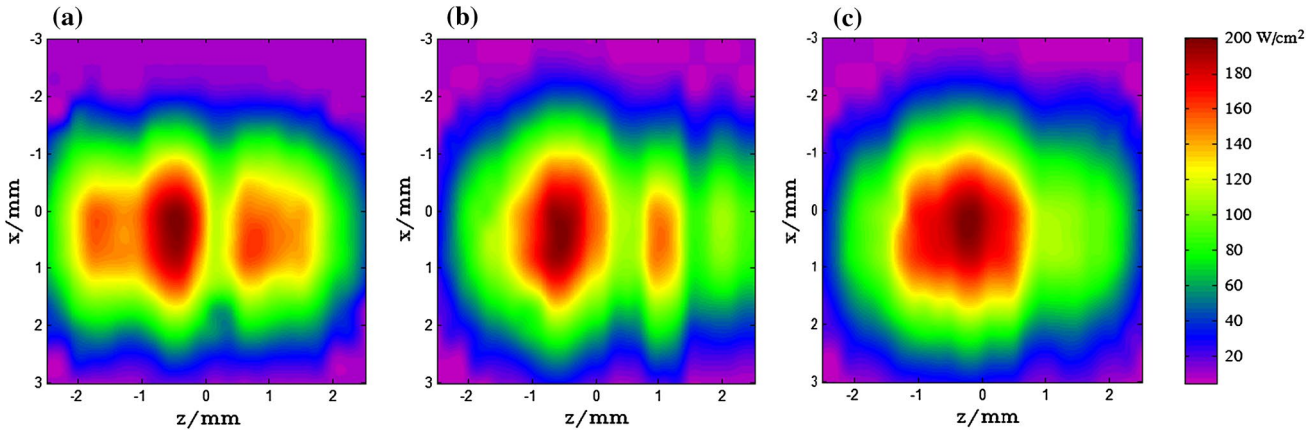

Fig. 7 Measured two-dimensional laser intensity distributions when flow velocity is **a** 1 m/s, **b** 2 m/s, and **c** 5 m/s

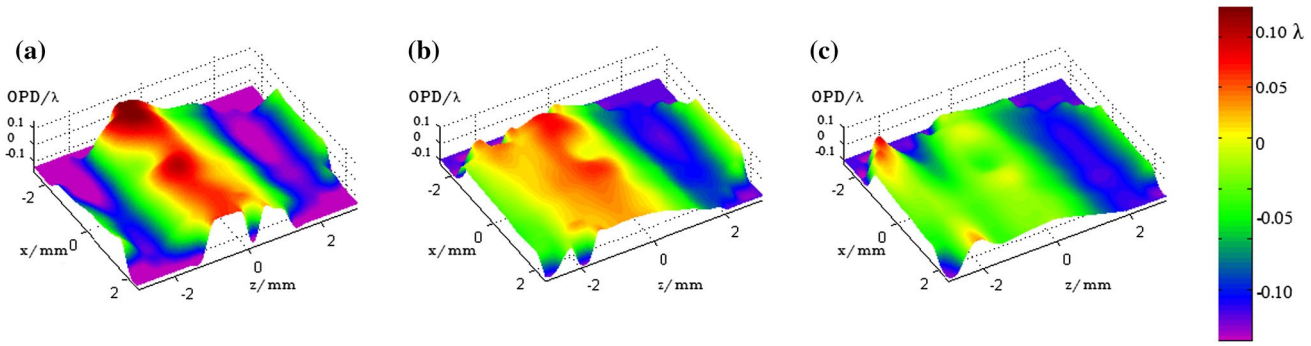

Fig. 8 Measured two-dimensional wavefront aberrations when flow velocity is **a** 1 m/s, **b** 2 m/s, and **c** 5 m/s

Table 1 Zernike polynomial coefficients of measured wavefront aberrations

Flow velocity	Zernike polynomial coefficients
1.00 m/s	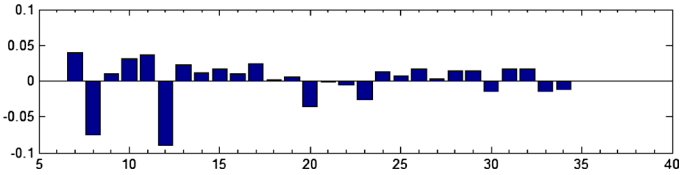
2.00 m/s	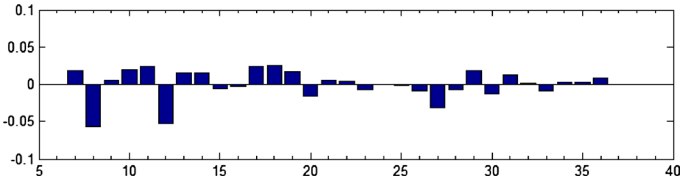
5.00 m/s	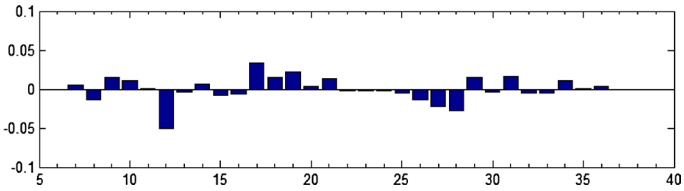

flow velocity with high turbulent intensity can reduce the aberration.

More detailed information of the optical aberration can be found by studying the coefficients of the Zernike polynomial expansion, as summarized in Table 1. The Zernike polynomial is expanded up to the 36th order. With the increase of turbulent flow velocity, the Zernike polynomial coefficients reduce generally. For the case with a flow velocity of 1 m/s, the coefficients of seventh-order to 15th-order Zernike polynomials take the leading role in the wavefront aberrations, while for the case of flow velocity of 5 m/s, the coefficients of seventh-order to 15th-order Zernike polynomials no longer have a dominant position. It is observed that with the increase in flow velocity, the dominant coefficients of wavefront aberrations transfer from low-order Zernike polynomials to more other Zernike polynomials. Moreover, the low-order Zernike polynomial corresponds to the aberration with low spatial frequency and large spatial scale. This may imply that the eddies with large-scale break up and eddy size decreases at high flow velocity.

The root mean square (RMS) values and the peak-to-valley (PV) values of the beam wavefront are used to evaluate the distortion degree of the beam. The sampling of RMS values and the PV values of the beam wavefronts has been conducted for 180 s. The RMS values and PV values versus time when flow velocity $u_0 = 1$, 2 and 5 m/s are shown in Figs. 9 and 10, respectively. The time-average values of RMS and PV decrease with the increasing flow velocity, showing a weakening of statistical average distortion degree. The specific time-average values and time-variance values of RMS and PV are demonstrated in Table 2. The time-variance values of RMS and PV decrease with increased flow velocity, which indicates that the irregular degree of distortion becomes weakened.

The wavefront phases at three feature points have been investigated. The three feature points consist of a location that has the highest power density (A) and two locations that have half of the power density (B and C), which are demonstrated in Fig. 11. The sampling of phase values of the three feature points has been conducted for 60 s. The phase values versus time when flow velocity $u_0 = 1$, 2 and 5 m/s are shown in Fig. 12. The specific measurement results of the time-variance phase values at three feature points are demonstrated in Table 3. The time-variance phase values of three feature points all decrease with increased flow velocity, indicating the phase values of beam wavefront tend to be stable.

The beam quality M^2 of the laser output versus the turbulent flow velocity is illustrated in Fig. 13. The beam quality M^2 is 8.8 and 14.3 in the x and z direction when the flow velocity is 1 m/s. The beam quality gets better as the turbulent flow velocity increases, and reduces to 7.9 and 12.7 in the x and z direction at the flow velocity of 5 m/s. The beam quality improves slightly with the increasing flow velocity. The multimode beam profile is due to the characteristic of stable cavity with large Fresnel number and the liquid aberrations in the cavity. A better beam quality of the laser output would be produced from an unstable cavity that has a strong ability of mode selection.

4 Conclusion

In conclusion, by using large-eddy simulation model and integrating the thermal-induced variations of refractive

index, we have numerically calculated the wavefront aberration induced by the turbulent flow, indicating that the fast turbulent flow velocity with high Reynolds numbers can reduce the aberration. We demonstrate a liquid-convection-cooled Nd:YAG disk laser oscillator. A output power of 30.7 W is produced at the pump power of 265 W,

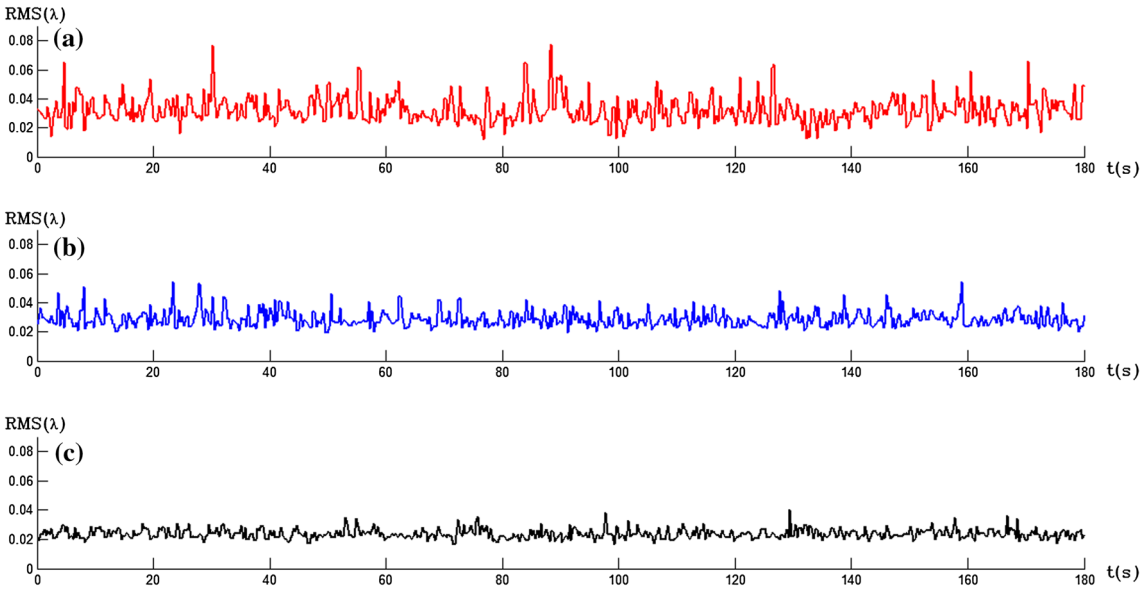

Fig. 9 Sampled RMS values of the beam wavefronts versus time when flow velocity is **a** 1 m/s, **b** 2 m/s, and **c** 5 m/s

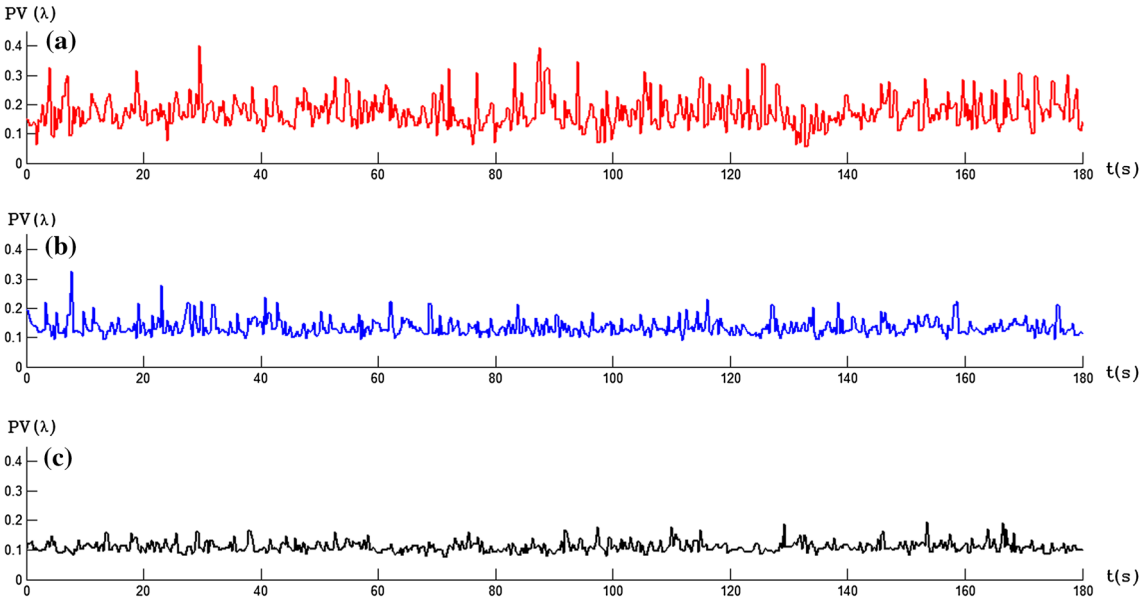

Fig. 10 Sampled PV values of the beam wavefronts versus time when flow velocity is **a** 1 m/s, **b** 2 m/s, and **c** 5 m/s

Table 2 Measured time-average values and time-variance values of the sampled RMS and PV

Flow velocity (m/s)	Time-average value of RMS (λ)	Time-variance value of RMS (λ)	Time-average value of PV (λ)	Time-variance value of PV (λ)
1.00	0.0320	0.0094	0.1728	0.0529
2.00	0.0283	0.0057	0.1358	0.0284
5.00	0.0231	0.0034	0.1140	0.0189

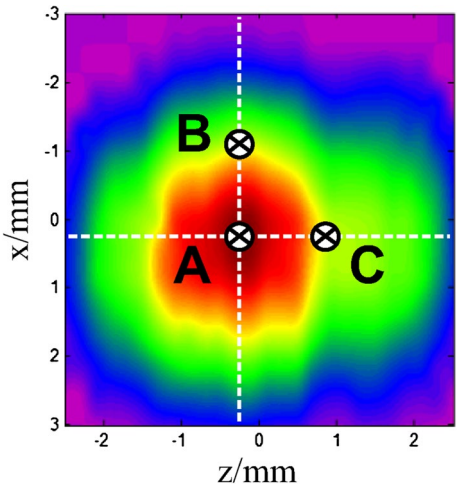

Fig. 11 Three feature points that consist of a highest power density point (*A*) and two half power density points (*B* and *C*)

corresponding to a optical–optical efficiency of 11.6 % and a slope efficiency of 14.1 %. The limitation of the output power is mainly due to the absorption loss in liquid layer and the thermal effect of the laser material. A higher output power can be obtained by reducing the thickness of the coolant liquid layer and enhancing the flow velocity of the flow field. A Shack–Hartmann wavefront sensor is used to measure the wavefront aberration and laser intensity distribution. Wavefront aberrations of the laser output at different coolant flow velocity are experimentally studied, and the RMS values as well as the PV values of the beam wavefront have been sampled. The experimental results reveal that, on the condition of turbulence cooling, enhancing the flow velocity and the turbulent intensity of coolant liquid can reduce the wavefront aberration of a laser oscillator.

The liquid-convection-cooled disk laser device with turbulence cooling can reduce thermal effects and withstand

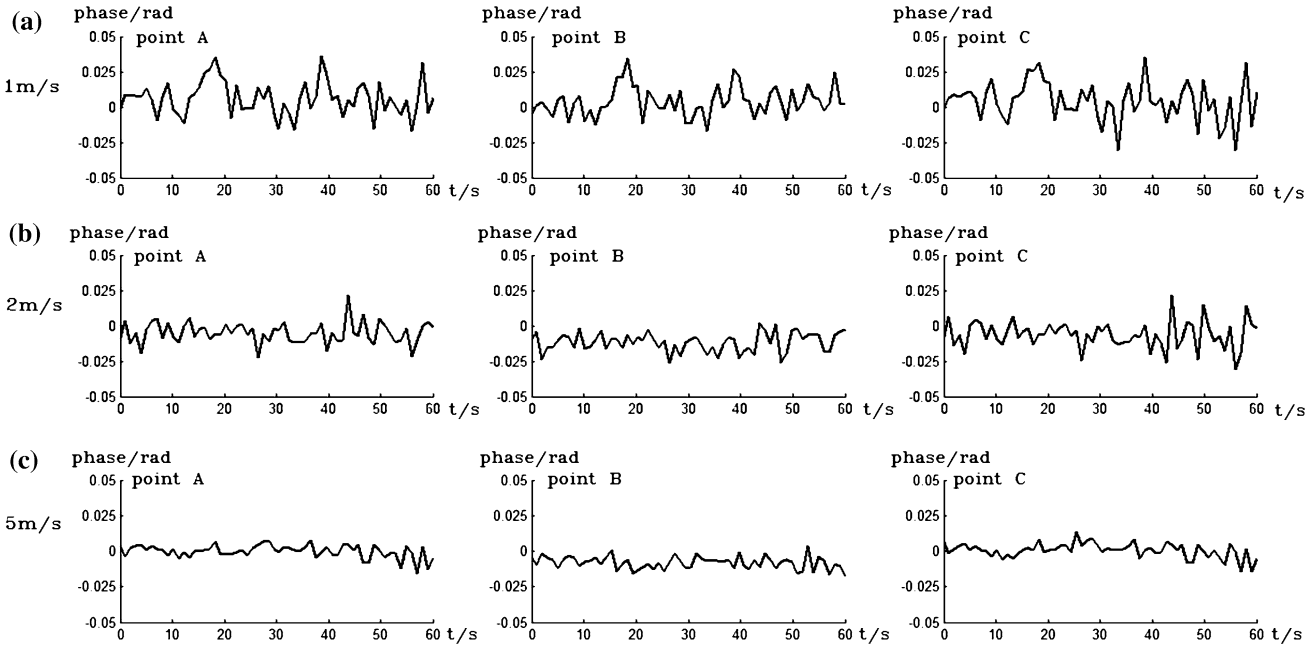

Fig. 12 Sampled phase values of the three feature points versus time when flow velocity is **a** 1 m/s, **b** 2 m/s, and **c** 5 m/s

Table 3 Measured time-variance phase values of the three feature points

Flow velocity (m/s)	Time-variance phase value of point A (rad)	Time-variance phase value of point B (rad)	Time-variance phase value of point C (rad)
1.00	0.01297	0.01601	0.01029
2.00	0.00846	0.01180	0.00771
5.00	0.00563	0.00570	0.00500

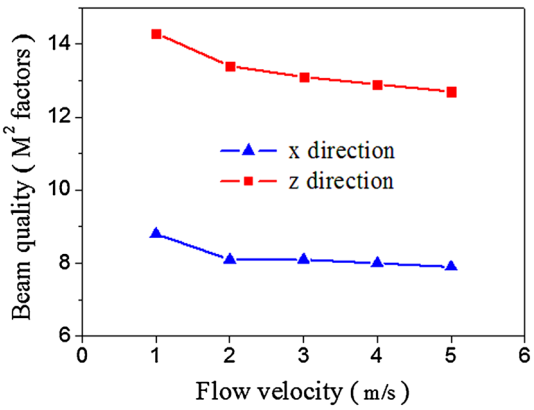

Fig. 13 Beam quality (M^2 factors) of the laser output versus the turbulent flow velocity

much higher pump power, since the convective heat transfer coefficient of the turbulent flow is much higher than that of the laminar flow. The experimental results presented in this paper verify that the method of high-speed turbulence cooling with excellent heat dissipation and weak wavefront aberration is suitable for high-power liquid-convection-cooled disk laser.

Acknowledgments The research was supported in part by Tsinghua University Initiative Scientific Research Program, in part by the National Natural Science Foundation of China (Grant 51021064), and in part by China Postdoctoral Science Foundation funded project (2013T60108).

References

1. S.J. McNaught, C.P. Asman, H. Injeyan, A. Jankevics, A.M. Johnson, G.C. Jones, H. Komine, J. Machan, J. Marmo, M. McClellan, R. Simpson, J. Sollee, M.M. Valley, M. Weber, S.B. Weiss, 100-kW Coherently Combined Nd:YAG MOPA Laser Array, in Frontiers in Optics, OSA Technical Digest (CD) (Optical Society of America, 2009), paper FThD2
2. E.I. Moses, R.N. Boyd, B.A. Remington, C.J. Keane, R. Al-Ayat, The national ignition facility: ushering in a new age for high energy density science. Phys. Plasmas **16**, 041006 (2009)
3. W. Koechner, *Solid-State Laser Engineering*, 6th edn. (Springer, Berlin, 2006)
4. M. Ostermeyer, D. Mudge, P.J. Veitch, J. Munch, Thermally induced birefringence in Nd:YAG slab lasers. Appl. Opt. **45**, 5368 (2006)
5. V. Sazegari, M.R.J. Milani, A.K. Jafari, Structural and optical behavior due to thermal effects in endpumped Yb:YAG disk lasers. Appl. Opt. **49**(36), 6910–6916 (2010)
6. Y. Lumer, I. Moshe, A. Meir, Y. Paiken, G. Machavariani, S. Jackel, Effects of thermally induced aberrations on radially and azimuthally polarized beams. J. Opt. Soc. Am. B. **24**(9), 2279–2286 (2007)
7. K.L. Schepler, R.D. Peterson, P.A. Berry, J.B. McKay, Thermal effects in Cr2+:ZnSe thin-disc lasers. IEEE J. Quant. Elec. **11**(3), 713 (2005)
8. H. Okada, H. Yoshida, H. Fujita, M. Nakatsuka, Nd: YAG split-disk laser amplifier for 10 J output energy. Opt. Commun. **260**, 277–281 (2006)
9. X. Fu, P. Li, Q. Liu, M. Gong, 3 kW liquid–cooled elastically-supported Nd:YAG multi-slab CW laser resonator. Opt. Express **22**, 18421–18432 (2014)
10. M.D. Perry, P.S. Banks, J. Zweiback, R.W. Schleicher, *Laser Containing a Distributed Gain Medium*. US Patent 7366, 211 B2 (2008)
11. A. Mandl, D.E. Klimek, Textron's J-HPSSL 100 kW ThinZag® Laser Program, in Conference on Lasers and Electro-Optics, OSA Technical Digest (CD) (Optical Society of America, 2010), paper JThH2
12. K.E. Oughstun, Aberration sensitivity of unstable-cavity geometries. J. Opt. Soc. Am. **3**(8), 1113–1141 (1986)
13. J.H. Ferziger, M. Perić, *Solution of the Navier–Stokes equations* (Springer, Berlin, Heidelberg, 2002)
14. X.Y. Luo, J.S. Hinton, T.T. Liew, K.K. Tan, LES modelling of flow in a simple airway model. Med. Eng. Phys. **26**(5), 403–413 (2004)
15. F. Felten, Y. Fautrelle, Y. Du Terrail, O. Metais, Numerical modelling of electromagnetically driven turbulent flows using LES methods. Appl. Math. Model. **28**(1), 15–27 (2004)
16. M.T. Landahl, E. Mollohristensen, *Turbulence and Random Processes in Fluid Mechanics*, 2nd edn. (Cambridge University Press, Cambridge, 1992)
17. J.W. Strohbehn, *Laser Beam Propagation in the Atmosphere* (Springer, Berlin, 1978)
18. M.E. Thomas, *Optical Propagation in Linear Media: Atmospheric Gases and Particles, Solid-State Components, and Water* (Oxford University Press, Oxford, 2006)